Kestrel Dual-Mesh Simulations for DPW-VII: Expanding the Envelope

Brent Pomeroy
NASA Langley Research Center
Configuration Aerodynamics Branch

CFD Drag Prediction Workshop VII
2022 AIAA AVIATION Forum
June 25-26, 2022

Outline

- **Kestrel Overview and Compute Environment**
- **Grids and Computational Methodology**
- **Selected Cases**
  - Case 1a: Grid Convergence Study
  - Case 2a: Alpha Sweep
  - Case 3: Reynolds Number Sweep
  - Case 4: RANS Grid Adaptation
  - Case 5: Beyond RANS (DDES with Grid Adaptation)
  - Extra credit interspersed throughout various Cases
- **Conclusions**

Kestrel CFD Solver

- **High-fidelity code from Department of Defense CREATE-AV**
  - Multidisciplinary tool that couples aerodynamics, S&C, thermochemistry, and propulsion
  - Cell centered
  - Includes RANS, URANS, and DDES schemes
  - Alpha-seeking for local time stepping
  - Alpha and C_L seeking for global time stepping
- **Inner/outer dual-mesh approach**
  - Static inner unstructured grid
  - Static or adaptive offbody Cartesian grid
  - Unstructured grid trimmed at constant distance
- **Executed with Kestrel 12.1 SDK**

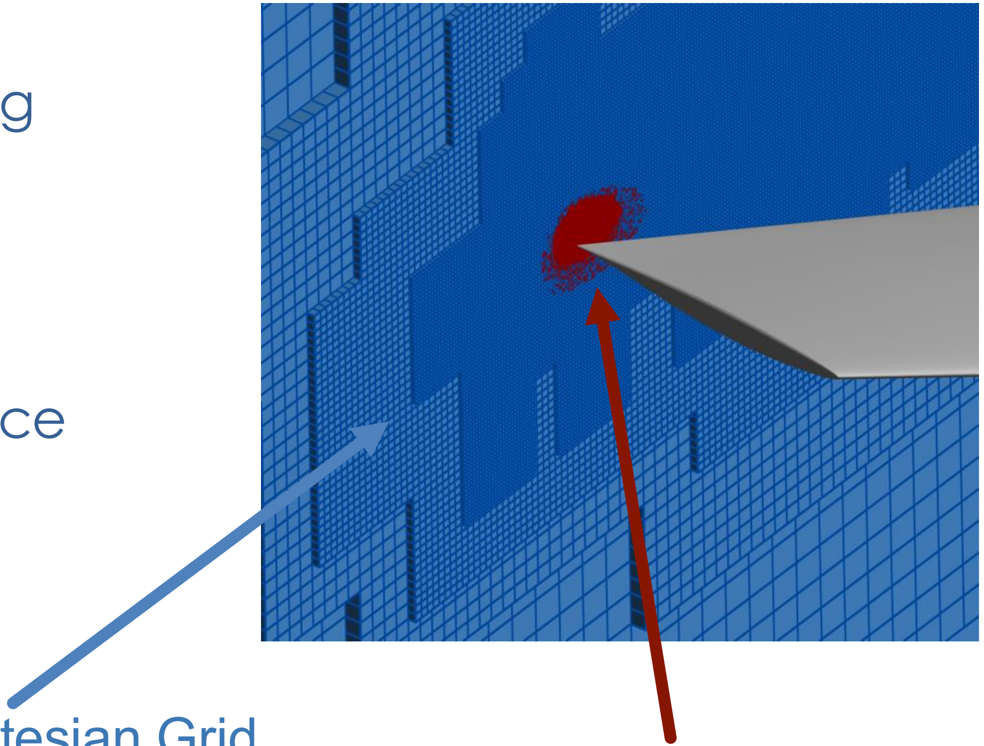

Supercomputing Environment

- **Executed on NASA Advanced Supercomputing (NAS) facility**
  - Comprised of four different supercomputers (Pleiades, Electra, Aitken, and Endeavour)
  - More than 11,000 nodes and 241,000 compute cores
  - Contains both Intel and AMD chips; TOSS3 (Linux 3) operating system
- **Resource usage for DPW-VII**
  - Intel Skylake nodes on Electra (a few select jobs on Haswell)
  - Between 1,600 and 3,200 processors
  - Walltime from a few hours to days
- **Total of 216 simulations**
  - Well in excess of 30 requested jobs for Cases 1a, 2a, 3, 4, and 5
  - Large number of runs due to significant additional investigation and alpha-searching

Grid Overview (1/2)

- **Committee-supplied JAXA unstructured grids**
- **Variety of aeroelastic deformations**
- **Six different grid densities**

	Tiny	Coarse	Medium	Fine	Extra Fine	Ultra Fine
Level	L1	L2	L3	L4	L5	L6
Approximate Cell Count	8.7×10^6	26.9×10^6	60.2×10^6	111.8×10^6	184.1×10^6	291.2×10^6

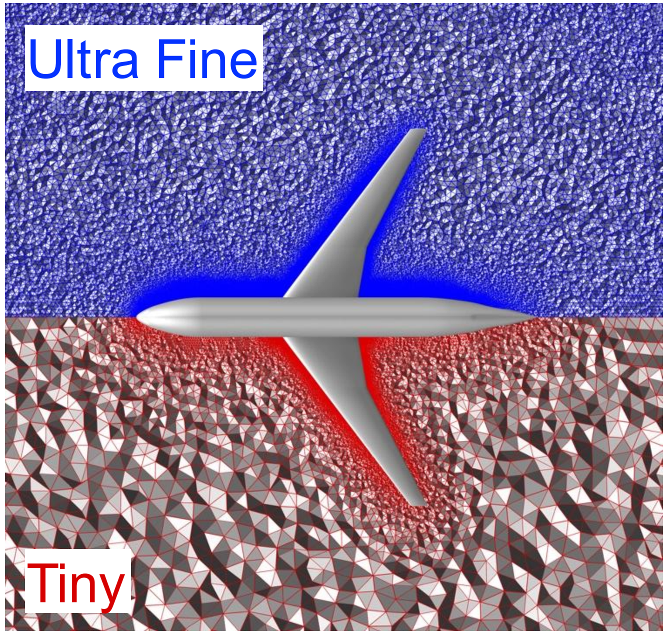

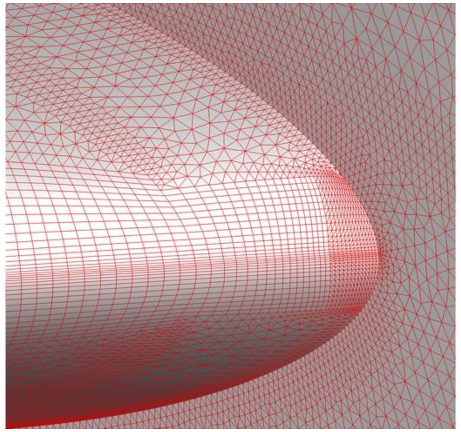

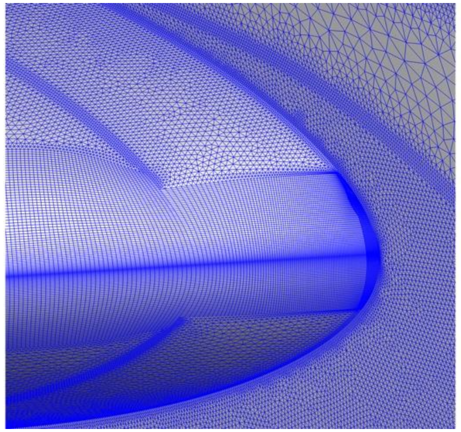

Grid Overview (1/2)

- Committee-supplied JAXA unstructured grids
- Variety of aeroelastic deformations
- Six different grid densities

	Tiny	Coarse	Medium	Fine	Extra Fine	Ultra Fine
Level	L1	L2	L3	L4	L5	L6
Approximate Cell Count	8.7×10^6	26.9×10^6	60.2×10^6	111.8×10^6	184.1×10^6	291.2×10^6

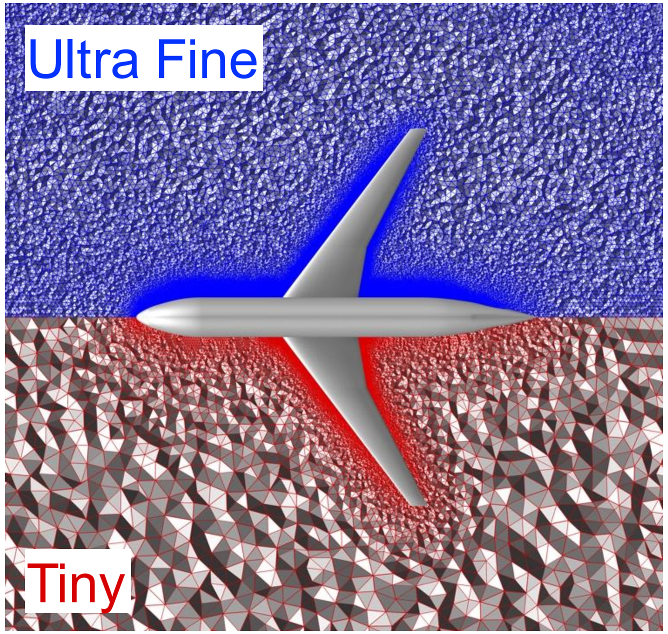

	Fully Unstructured	Adaptive Unstructured	Fixed Cartesian	Adaptive Cartesian
Case 1a	✓		✓	
Case 2a			✓	
Case 3			✓	
Case 4				✓
Case 5				✓

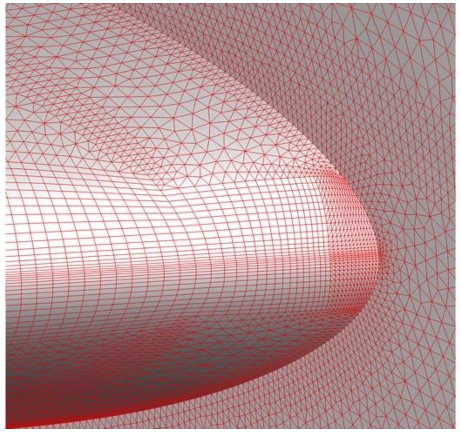

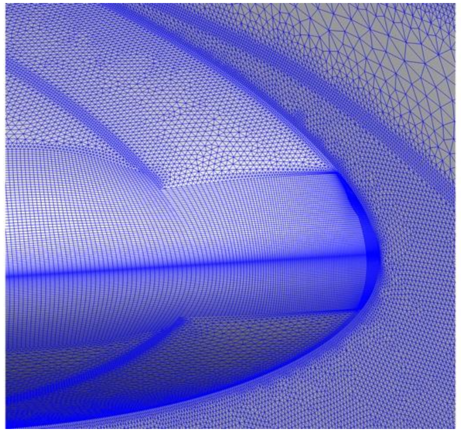

Grid Overview (2/2)

- **Mixed element surface and volume grid**
- **Surface grid made of quadrilaterals and triangles**
- **Volume grid included tetrahedron, pyramids, prisms, and hexahedron**

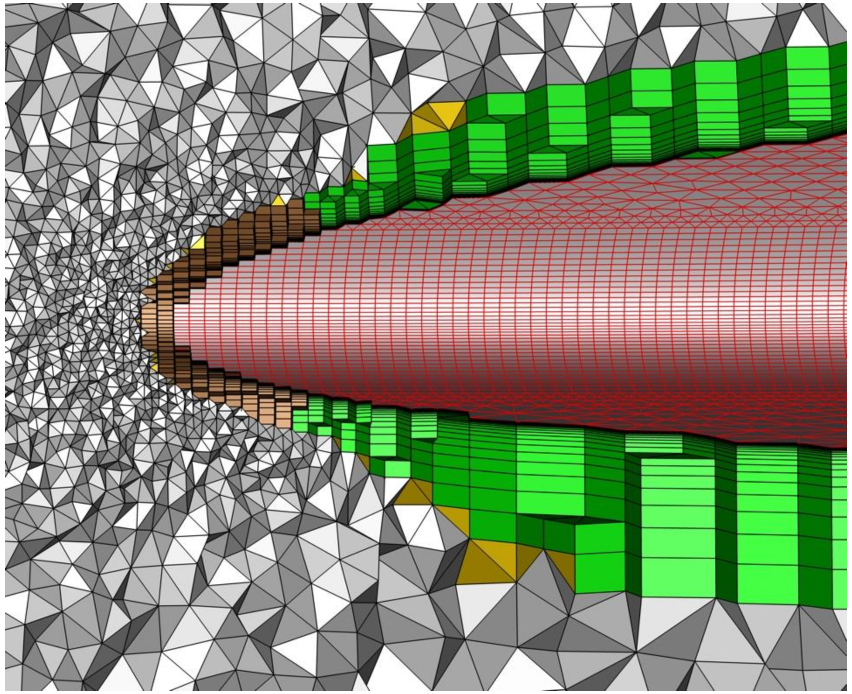

Surface

Red: quadrilaterals and triangles

Volume

Gray: tetrahedron
Gold: pyramids
Green: prisms
Brown: hexahedron

Solution Setup

- **Computational approach**
  - HLLE++ inviscid flux and LDD+ viscous flux
  - Second-order spatial and temporal accuracy
  - Temporal damping applied to inner and outer grid
  - Fully-turbulent SARC-QCR (QCR2000)
- **KCFD (inner solver) and SAMAir (outer solver)**
- **Executed all RANS cases to 20,000 iterations, regardless of convergence behavior**
- **Appreciation extended to the Committee for accelerating development of the reduction scripts and data file format**

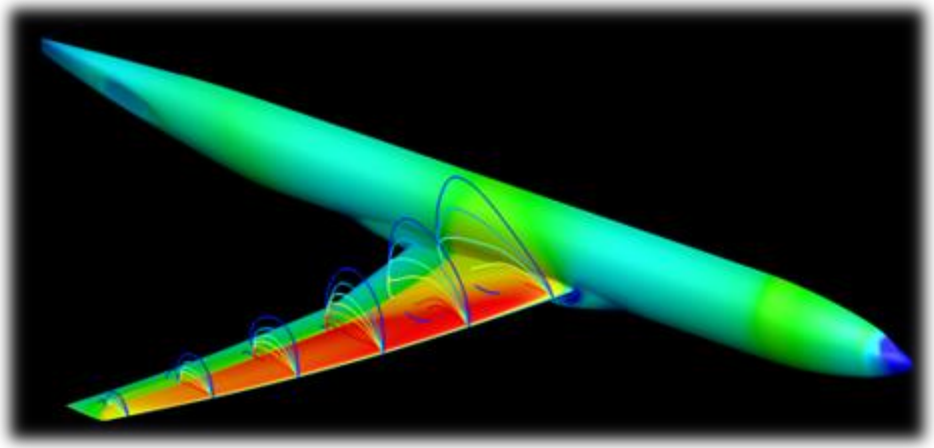

Case 1a: Unstructured Grid Convergence

Mach 0.85
Re = 20 million
C_L = 0.58

- **Simulations executed on all six densities**
- **Data averaged over last 2,000 iterations**
  - From user's best practices; may need more analysis
  - More stable grid convergence for coarser grids
  - Variations in C_L consistent with typical Kestrel results

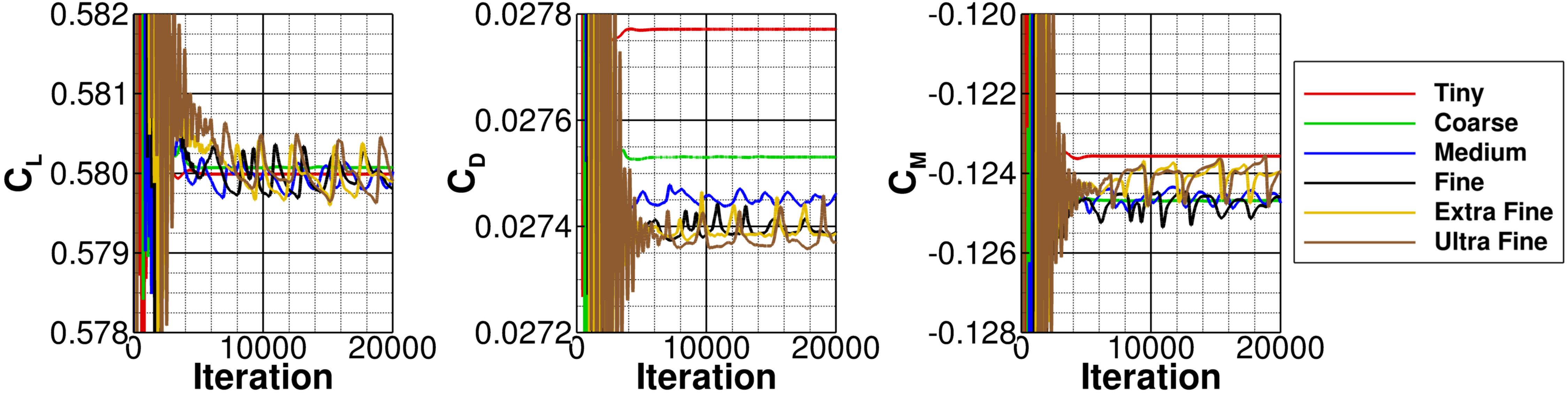

Case 1a: Unstructured Grid Convergence

- **Simulations executed on all six densities**
- **Data averaged over last 2,000 iterations**
  - From user's best practices; may need more analysis
  - More stable grid convergence for coarser grids
  - Variations in C_L consistent with typical Kestrel results
- **Excellent grid convergence with increasing density**

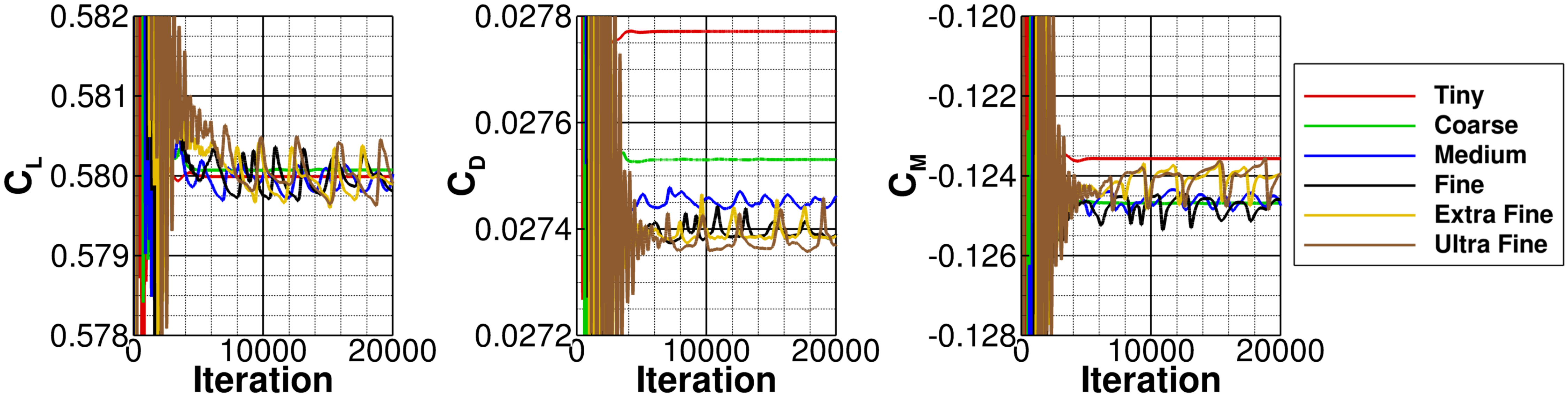

Case 1a: Inboard Pressure Cuts

- **Only minimal differences seen in inboard-most C_P cuts**
- **Largest differences seen at inboard cut trailing edge**
  - Region of interest for SOB separation region
  - Grid density has a large effect on the junction flow
- **Moderate deviations near the leading edge lower surface**
- **Decreased differences outside of junction flow region (Cut 5 plotted)**

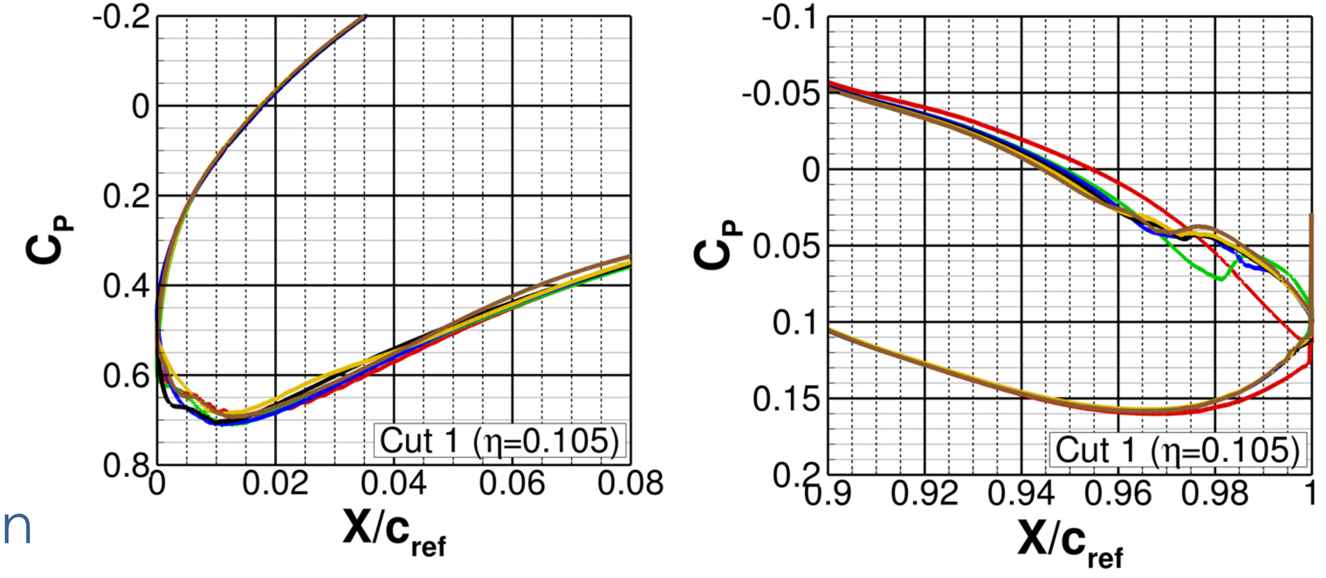

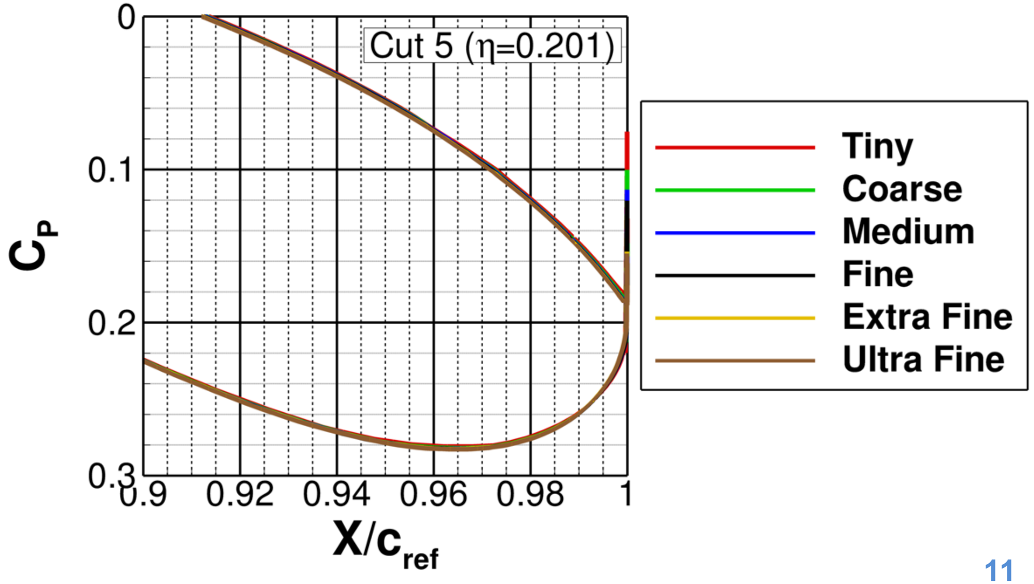

Case 1a: Midspan and Outboard Pressure Cuts

- **Few differences seen in shock strength or location for the midspan and outboard locations (Cuts 9 and 12 representative of all results)**
- **Minimal variations seen in trailing edge behavior (Cut 12 is representative)**

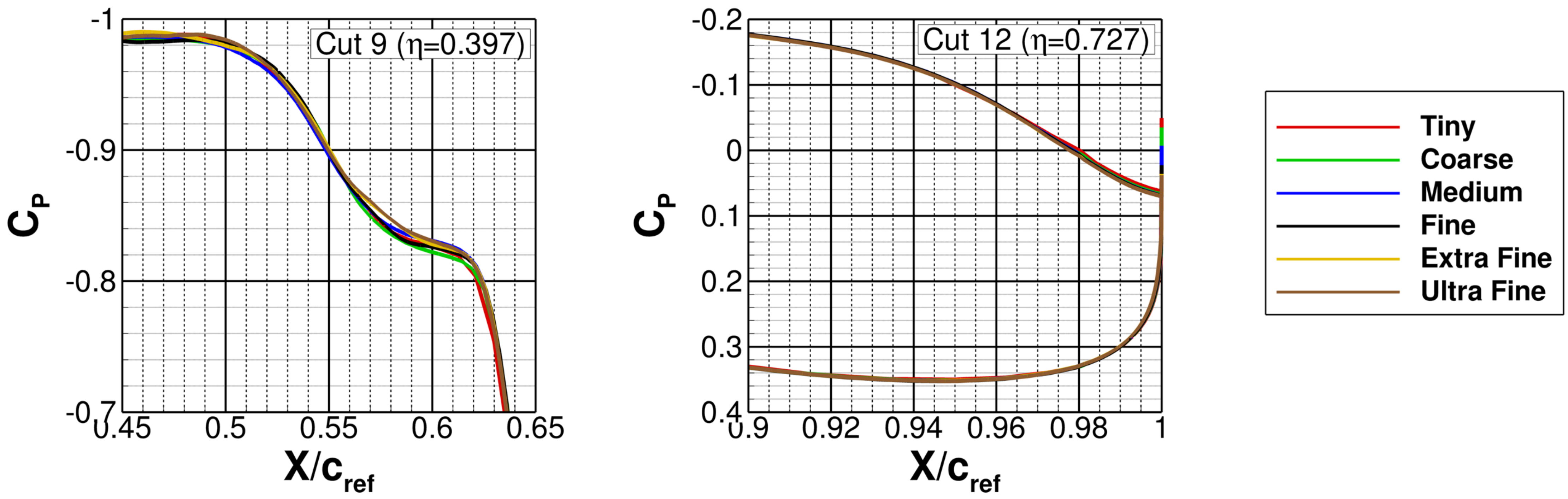

Case 1a: Overset Computational Domain

- Inner-most Cartesian cell size of outer unstructured cell (best practice)
- Outer box extends ~110 c_{ref} in all directions
- Cartesian growth rate automatically determined

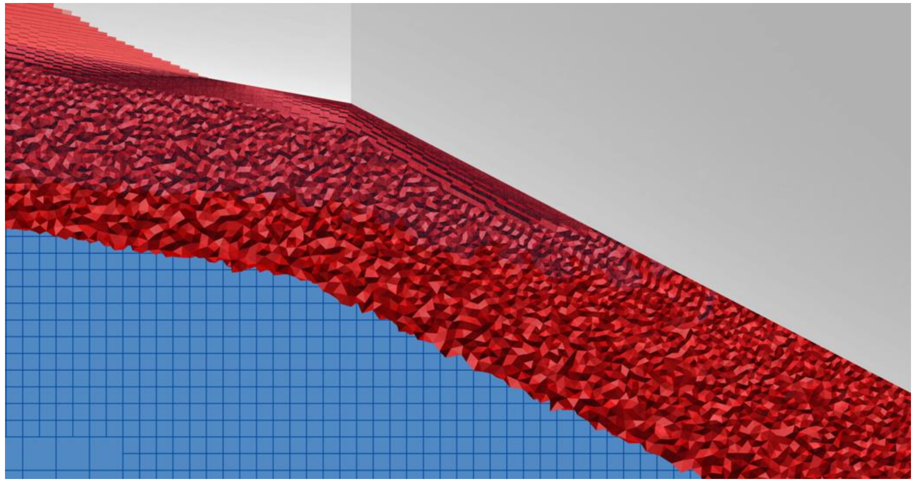

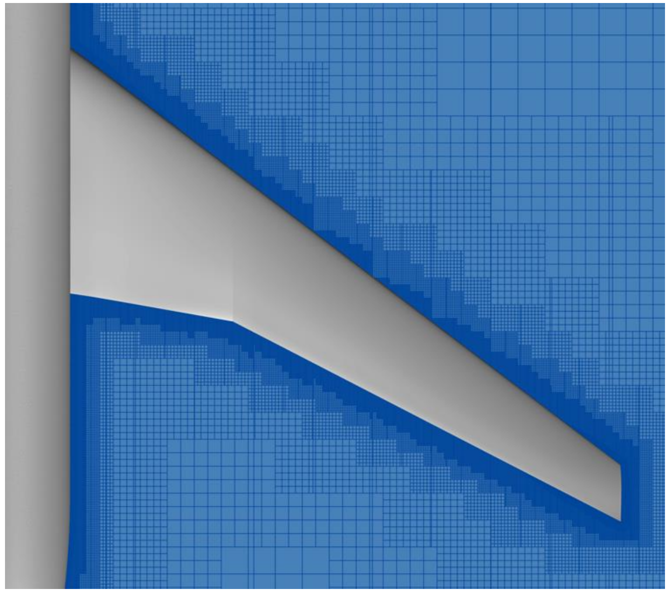

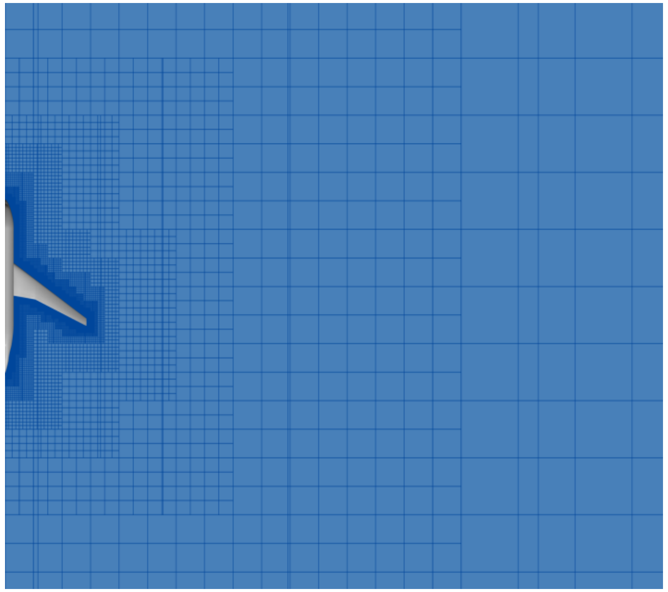

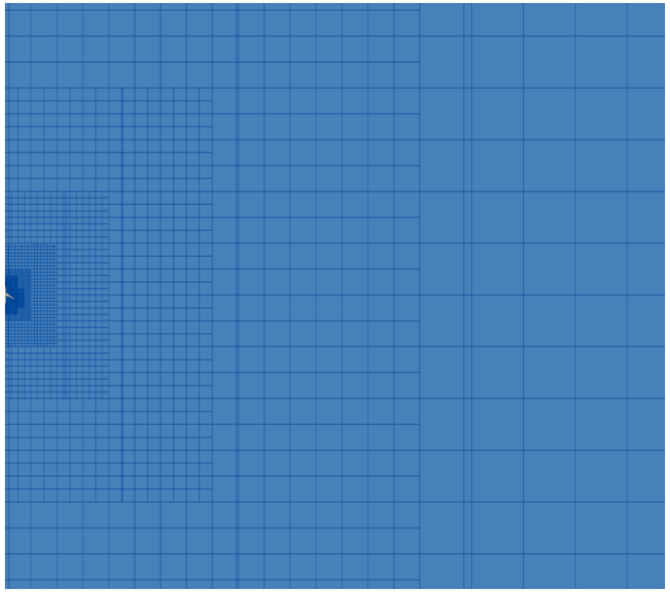

Case 1a: Trim Distance Study

- **Nearbody grids trimmed using carp**
  - Kestrel's grid manipulation package
  - Supports numerous grid formats (including ugrid)
  - Inner grid trimmed at a range of distances
- **Simulations were executed at constant α (2.758 deg.) with minimal difference in drag or convergence**

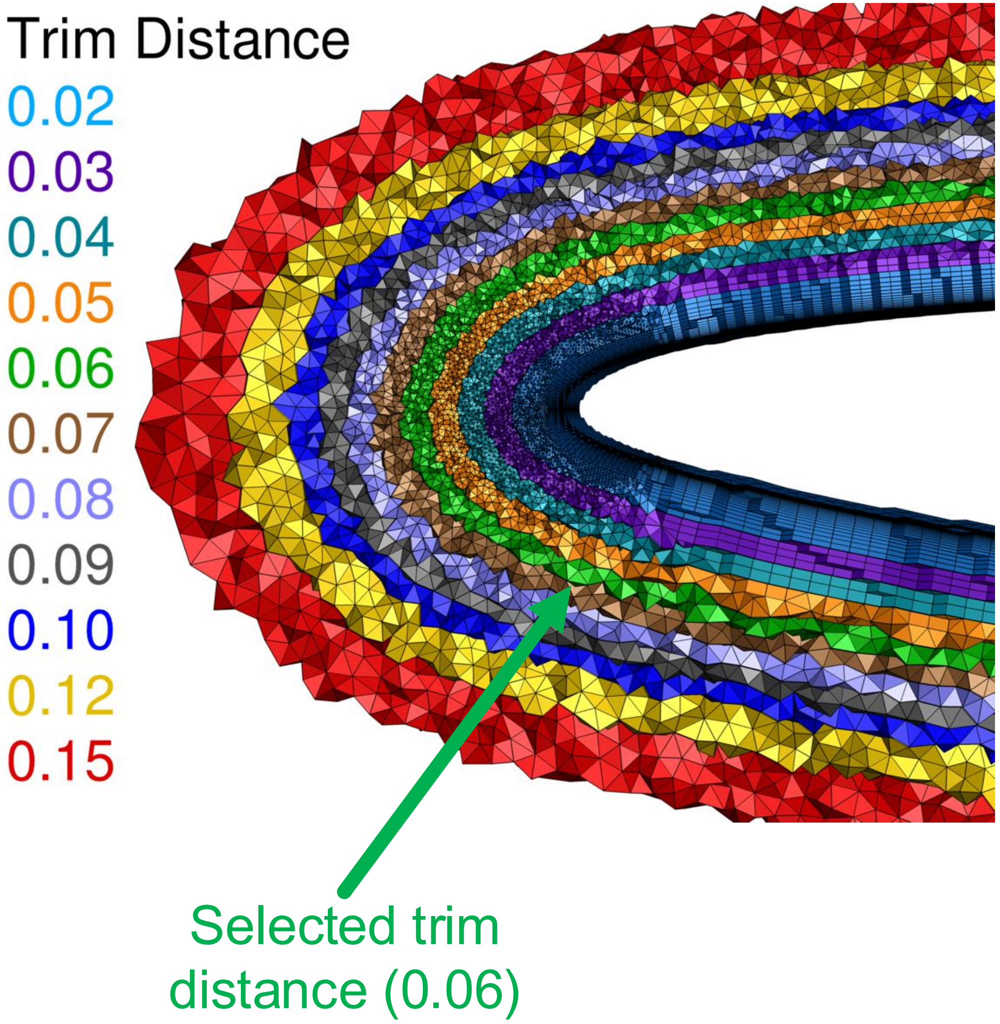

Case 1a: Trimmed Grid Visualization

- Selected 0.06
- Close trim distance can lead to erroneous results and solution instability
- Largely isotropic cell spacing at selected distance
- Trim distance held constant for subsequent solutions

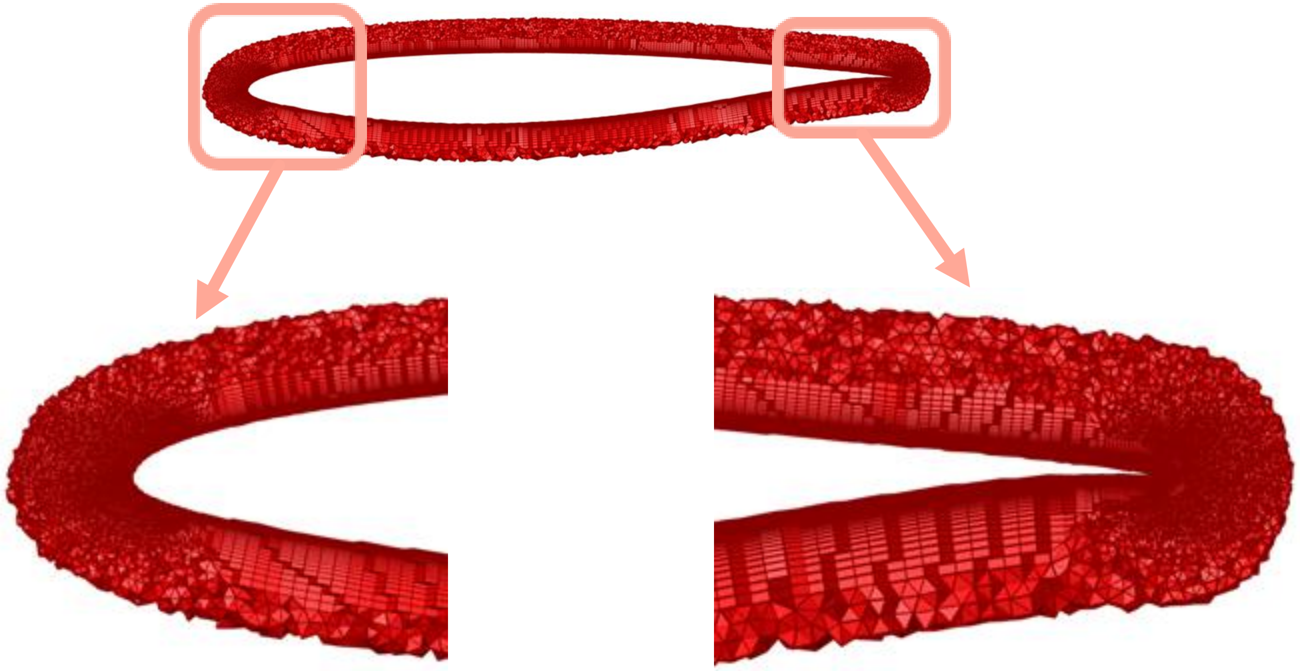

Case 1a: Aerodynamic Performance

- **Alpha sweep executed on tiny and medium/trimmed (baseline) grids**
  - Sweep from α of 0 to 8 deg. shown every 0.25 deg. (total of 86 jobs)
  - Tiny grid yields decreased $\alpha_{pitchup}$ and deeper C_M bucket (not shown)
- **Difference in inboard flow separation ~0.50 deg.**
- **Deviations observed in deep stall region**

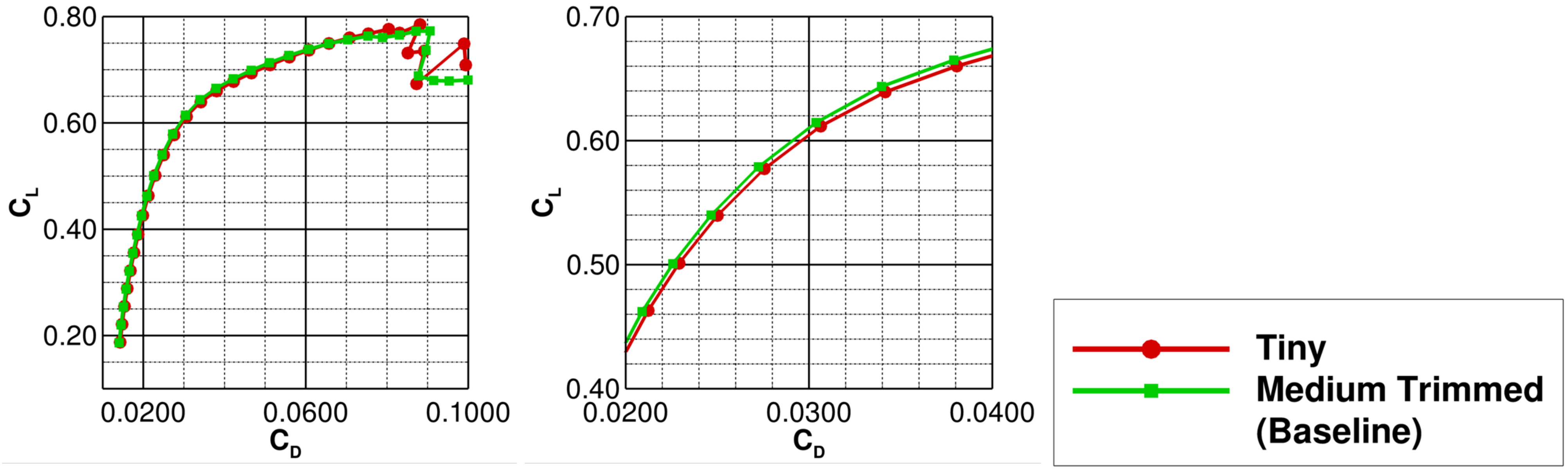

Case 1a: Aerodynamic Performance

- **Alpha sweep executed on tiny and medium/trimmed (baseline) grids**
  - Sweep from α of 0 to 8 deg. shown every 0.25 deg. (total of 86 jobs)
  - Tiny grid yields decreased $\alpha_{pitchup}$ and deeper C_M bucket (not shown)
- **Difference in inboard flow separation ~0.50 deg.**
- **Deviations observed in deep stall region**
- **C_D differences ~2.2 counts at α of 3.00 deg.**

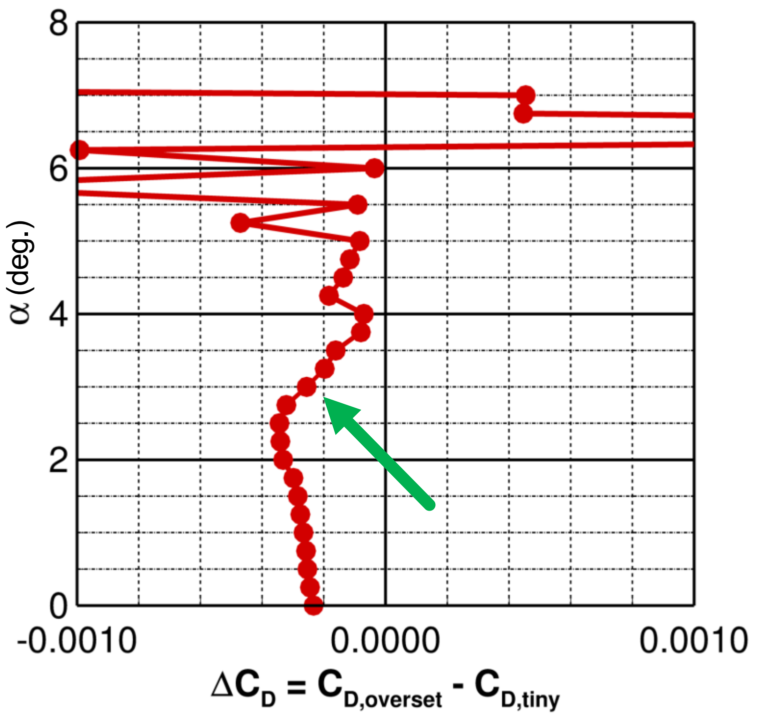

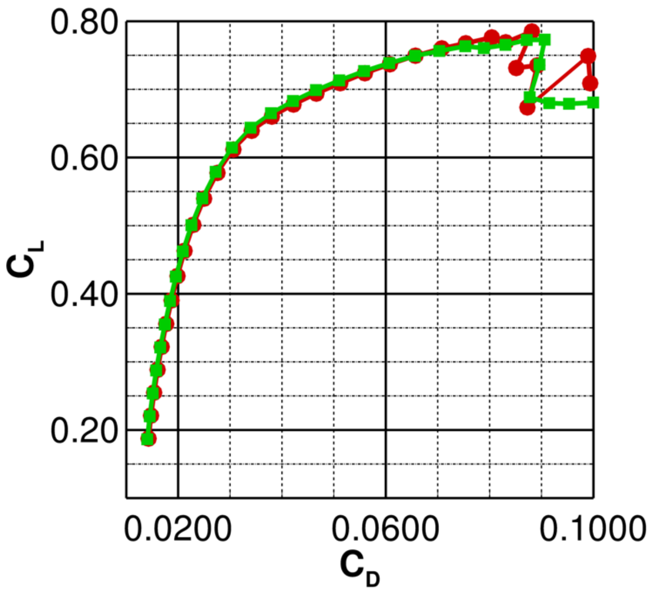

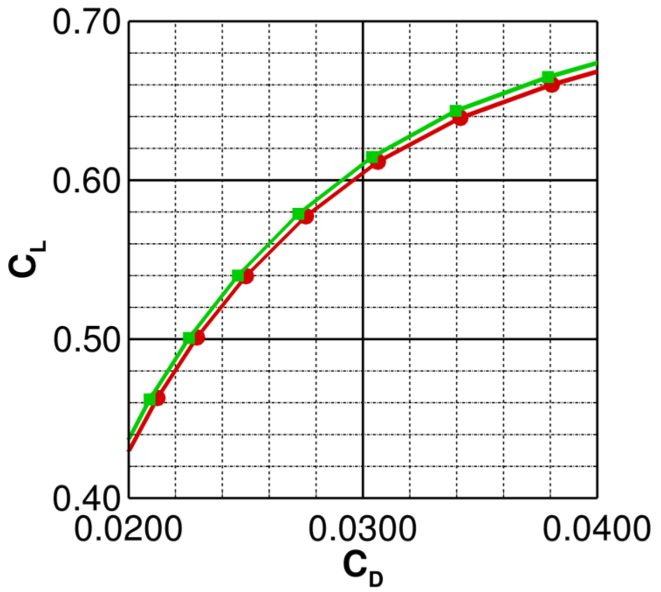

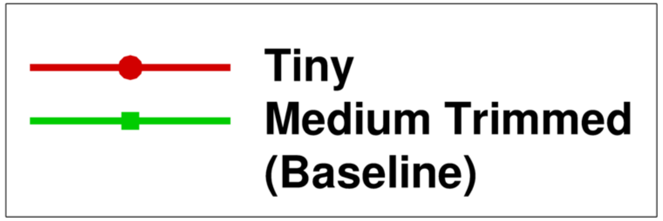

Case 1a: Computational Cost

- **Total cost for medium-density mesh**
  - Fully unstructured grid
  - Trimmed grid at 0.06
- **1600 CPUs (40 Skylake nodes)**
- **About 10.5 hours total for overset formulation**
- **Cost per iteration is primarily between 2 and 4 sec. (without refinement)**
- **Overset solution yields ~50% reduction in computational cost relative to unstructured**

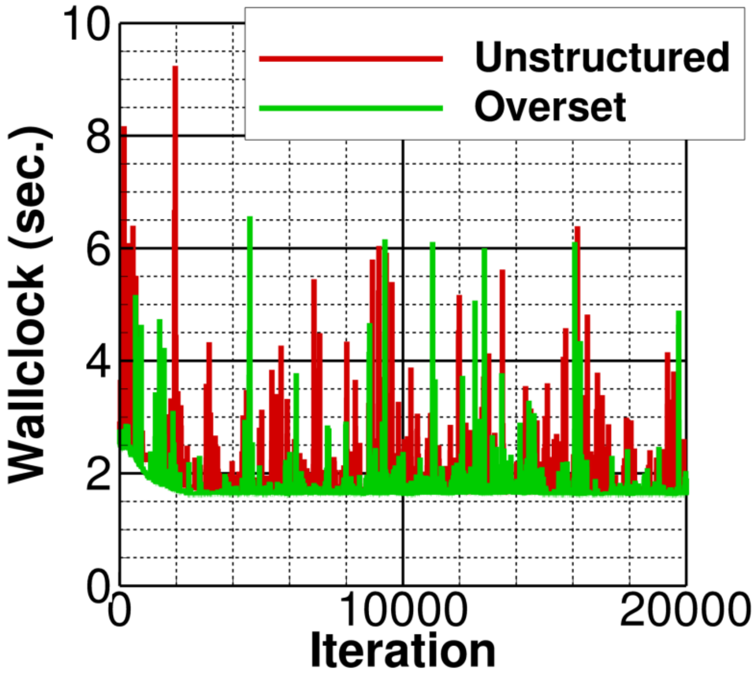

Case 1a: Medium Trimmed Grid Alpha Sweep

- **Pitch break at ~3.0 deg. (C_L ~0.62)**
- **Inboard wing separation at ~7.25 deg.**

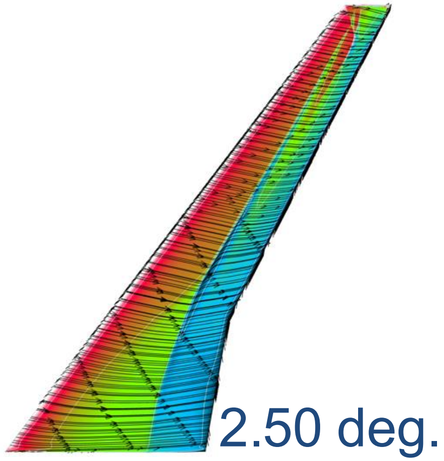

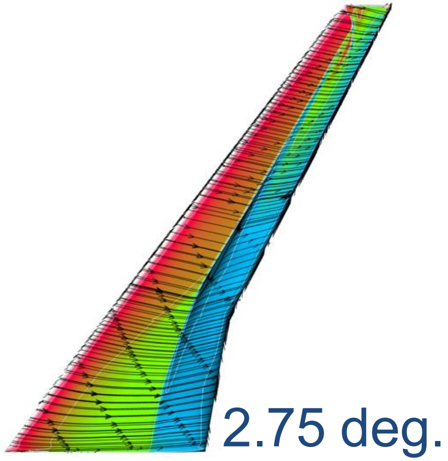

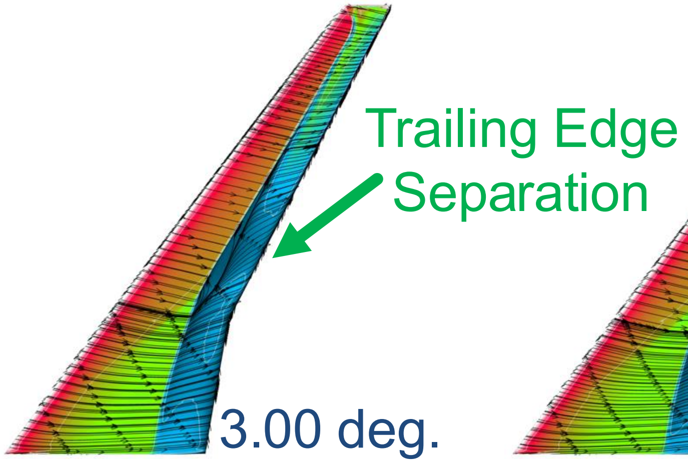

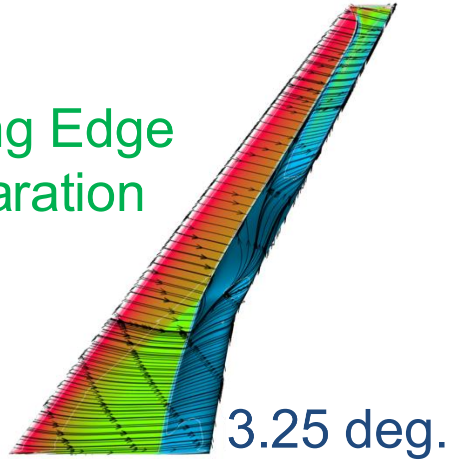

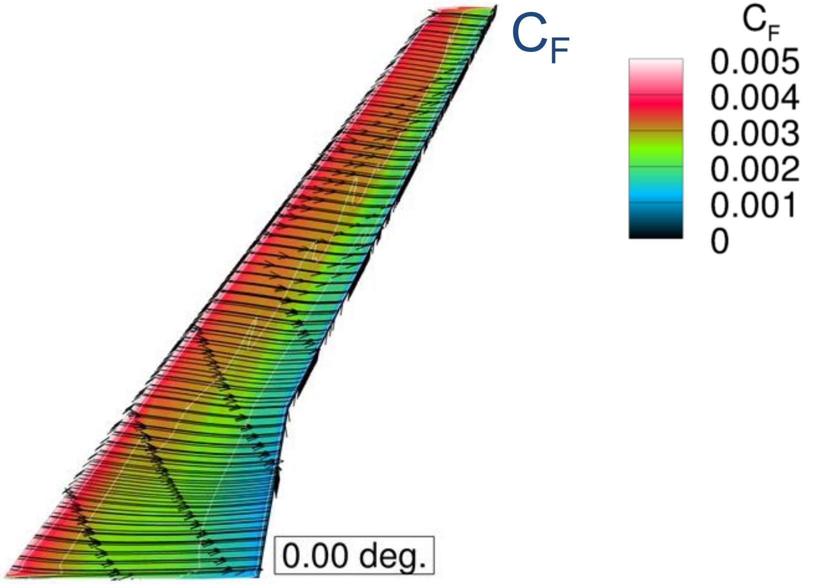

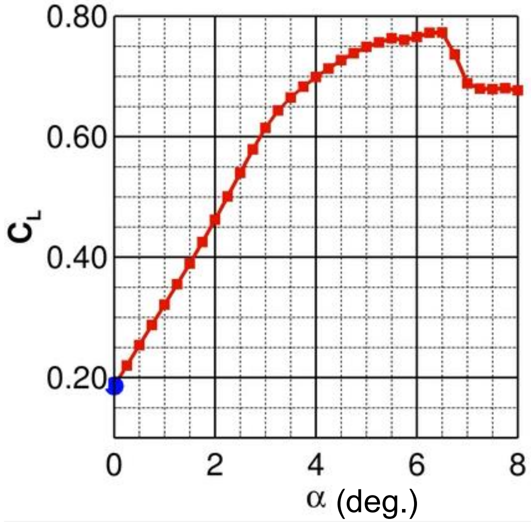

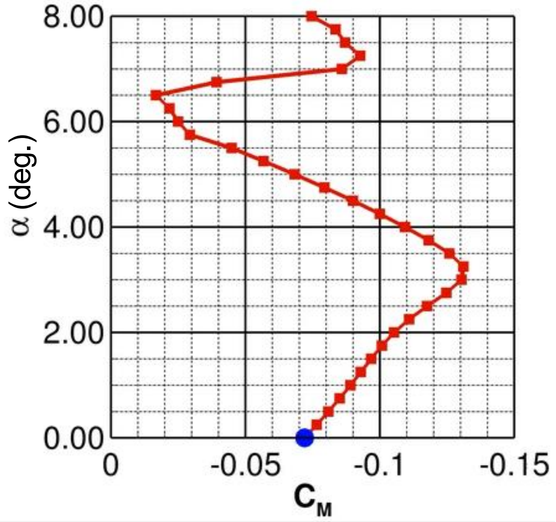

Case 2a: Polar

- Executed with medium grid and appropriate aeroelastic deformations
- Increasing flow separation observed for α > ~3.0 deg.
- Progressive decambering leads to monotonically-decreasing $C_{L\alpha}$ slope
- Pitching moment break observed near C_L ~0.62

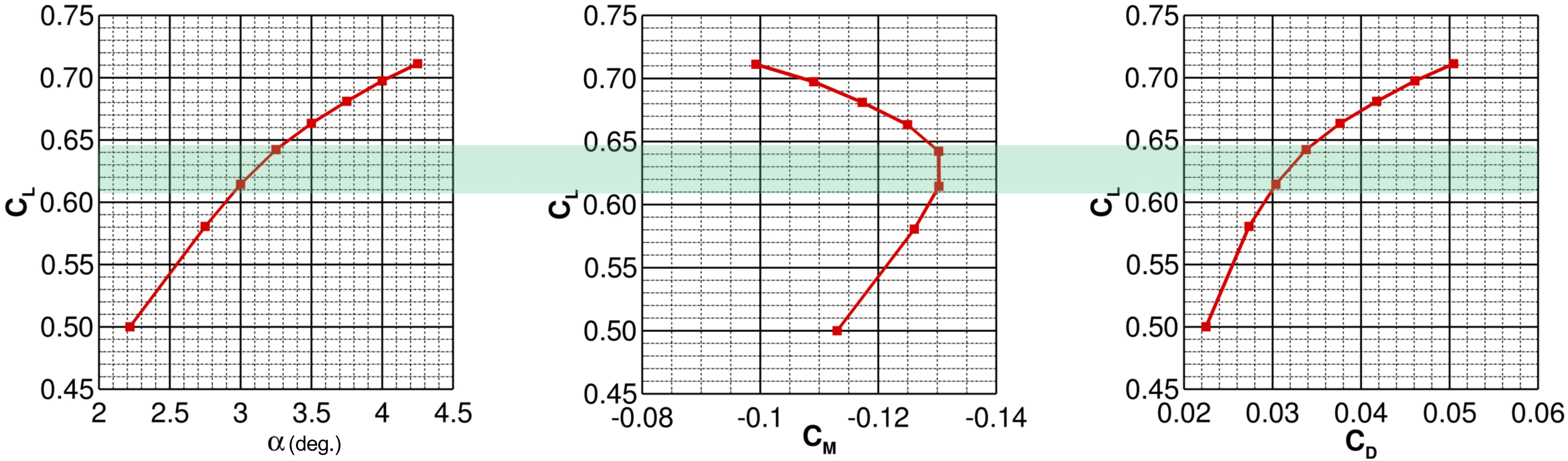

Case 2a: Inboard Surface Cuts

- Increasing angle of attack yields a downstream shift in shock location
- Shock clearly evidenced by C_P and C_F
- Flow nominally attached downstream of the shock
- Decelerated flow seen at trailing edge

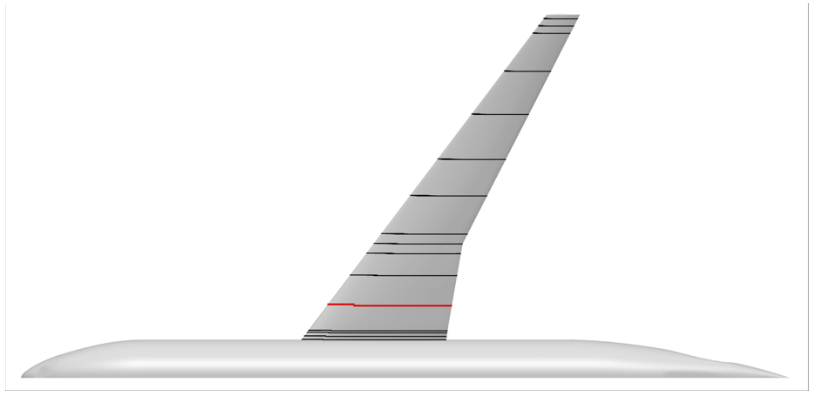

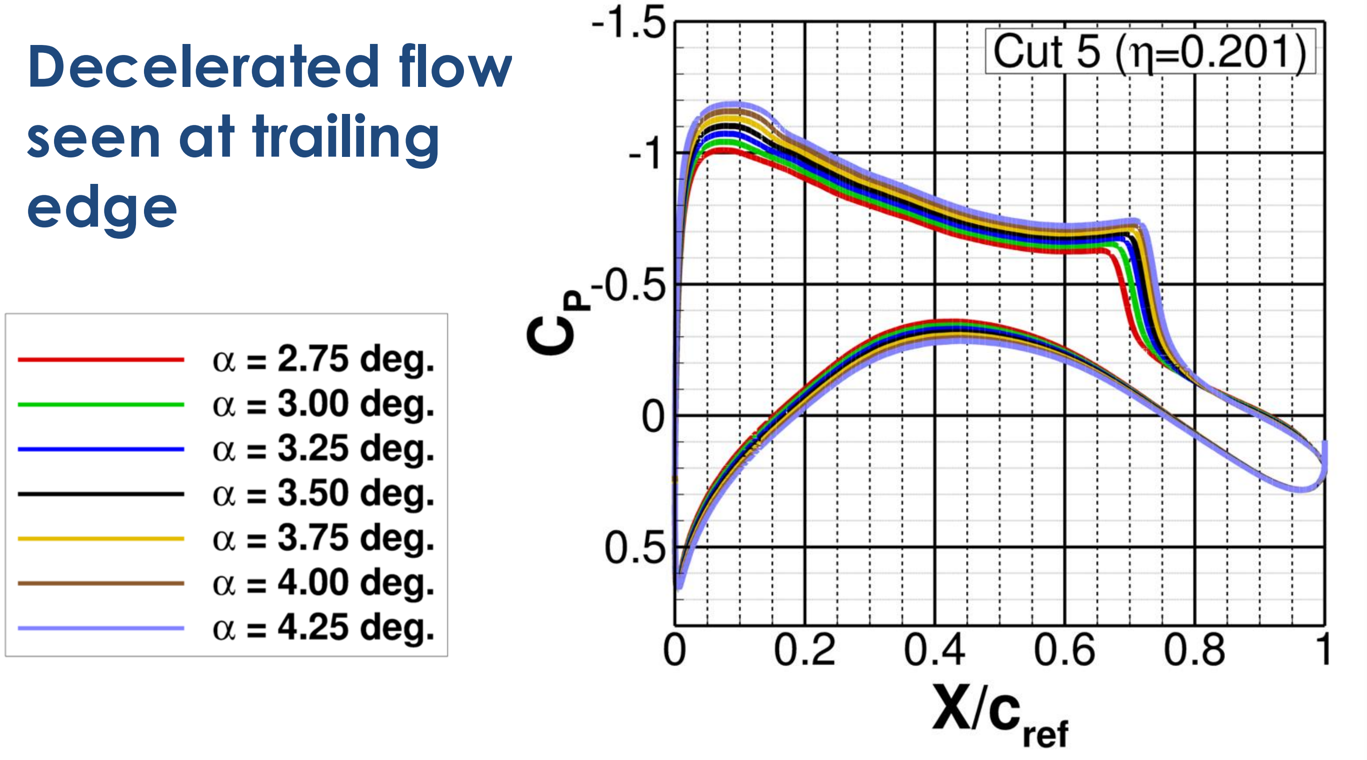

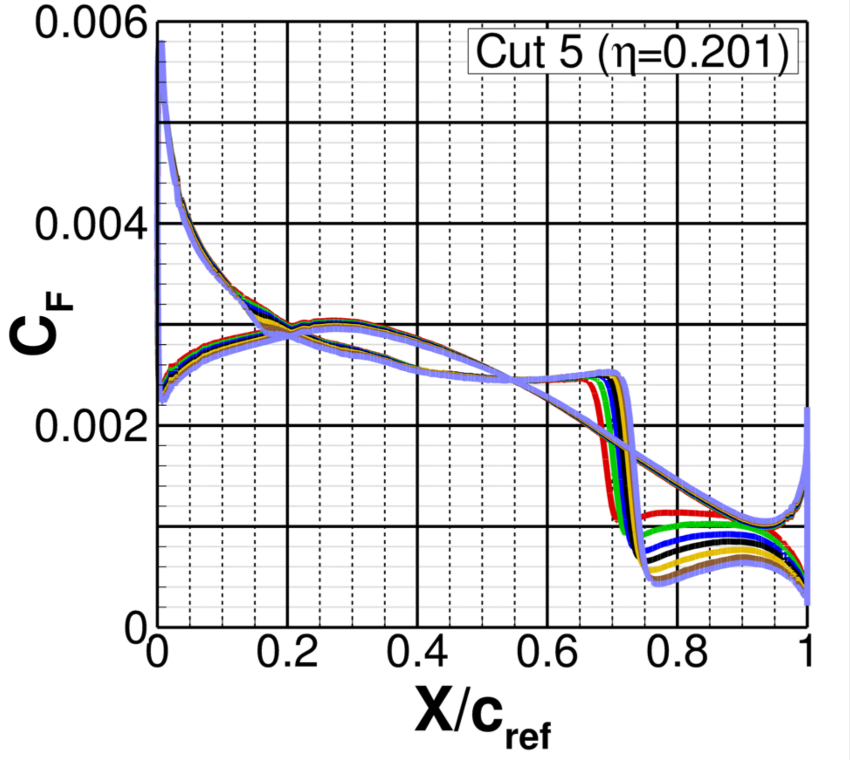

Case 2a: Mid-Span Surface Cuts

- Downstream shift in shock observed with larger angles of attack (expected)
- No double shocking at high angles
- Flow separates at shock location and fails to reattach above α = 3.25 deg.

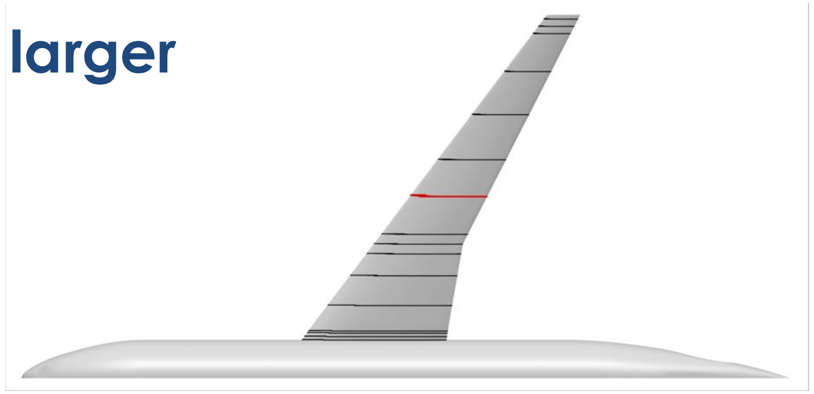

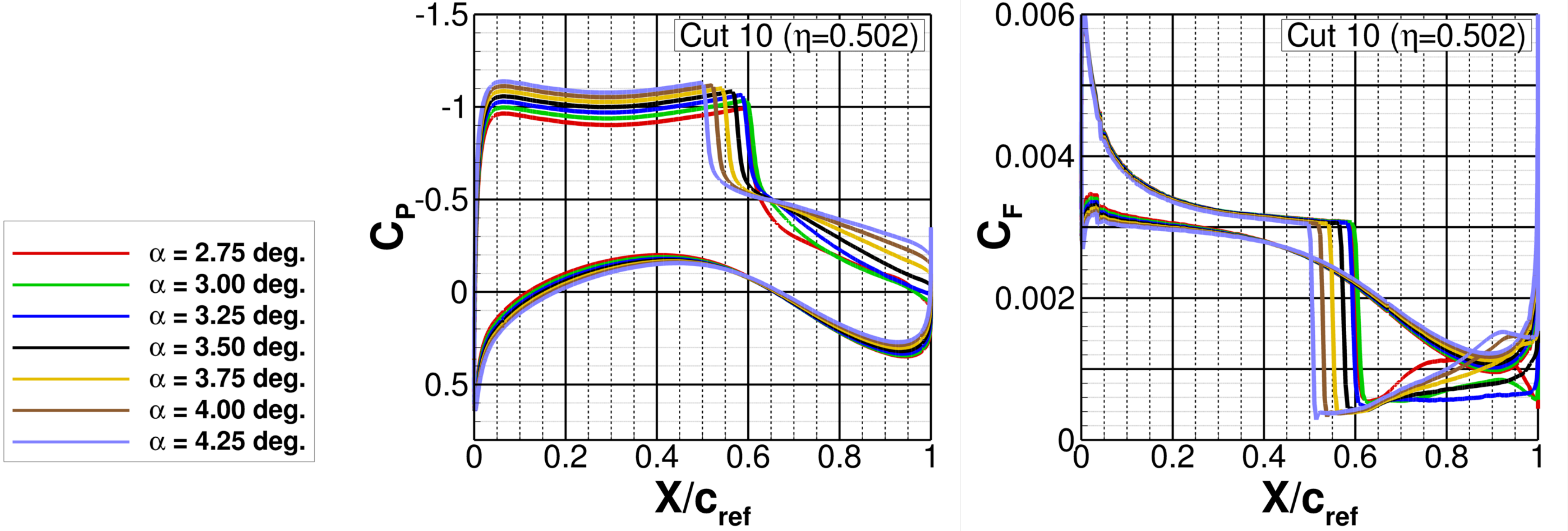

Case 3: Reynolds Number Sweep

- Executed on LoQ and HiQ lofts at $C_L = 0.50$
- Significant drag rise with decreased Re (expected)
- Large drag rise seen from Re of 20 million to 5 million (expected)

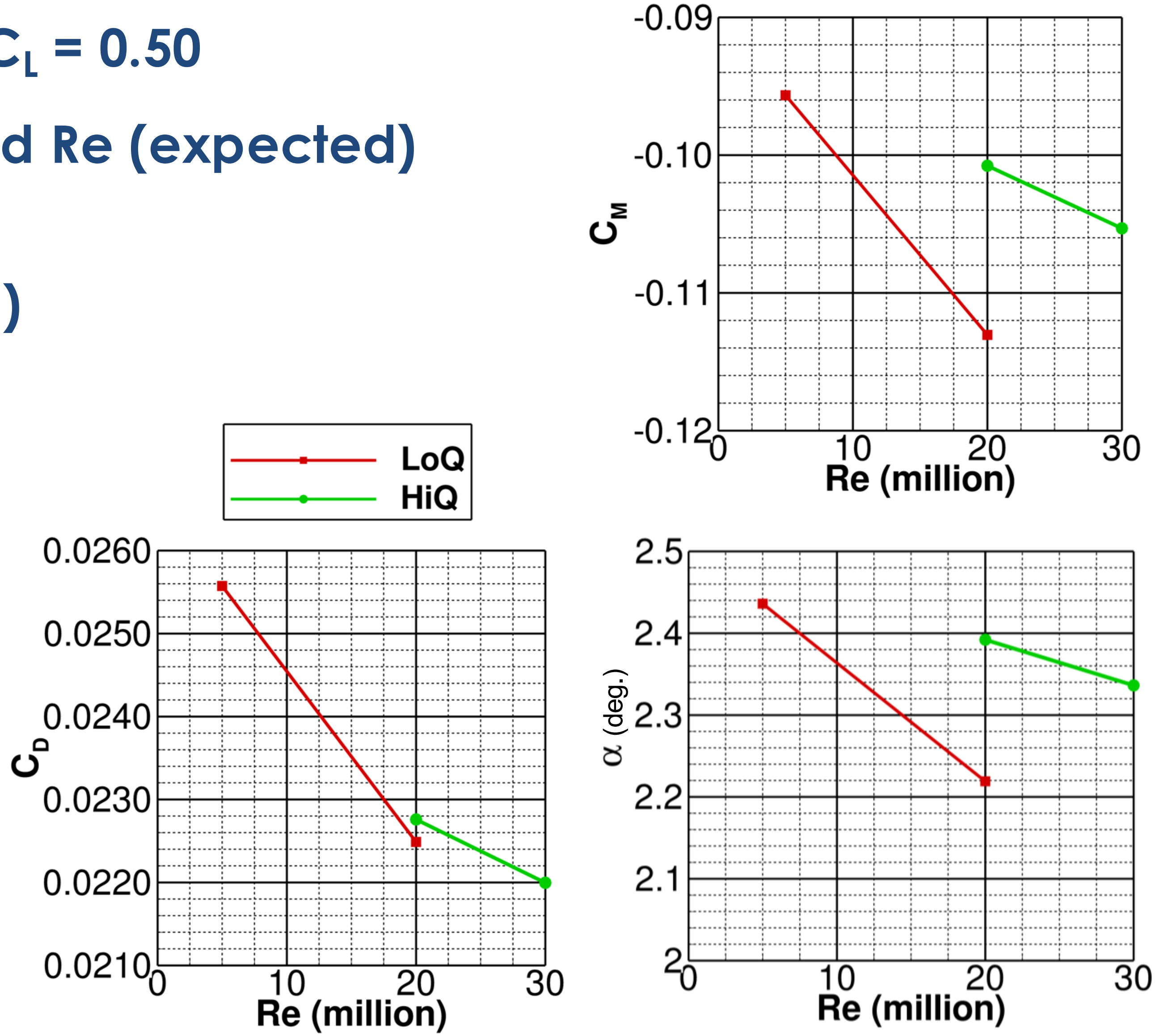

Case 4: RANS Adaptive Mesh

- **Adaptive mesh refinement performed in offbody Cartesian grid**
  - Nearbody-grid adaptation not yet available
  - User-specified region limits shown in blue box
  - Amount of refinement based upon a threshold value
  - Separated wake led to decision to refine based on ω
- **Refinement applied every 250 iterations**
- **Adaptation used over the entire simulation (not frozen)**
- **Grid density must be traded with computational cost**

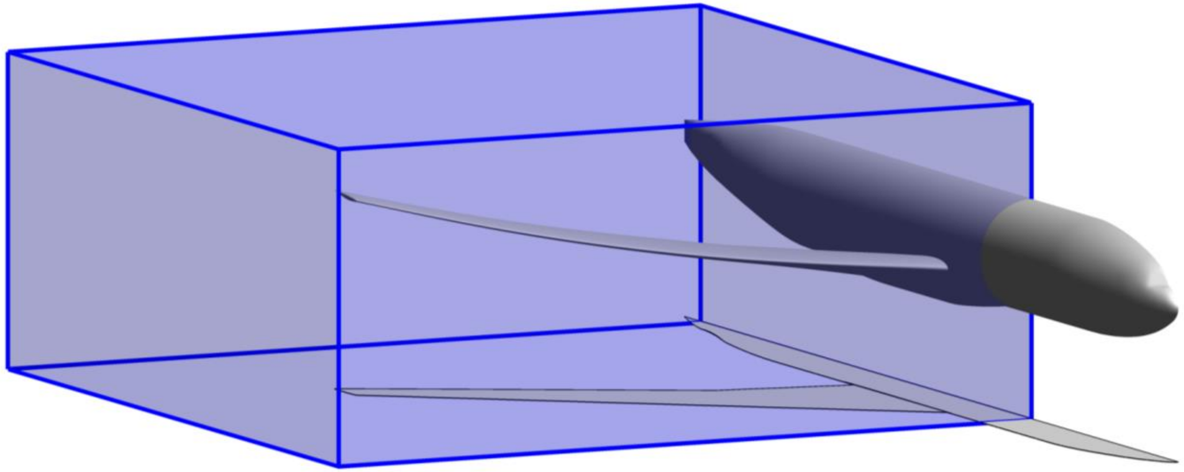

Case 4: Effect of Refinement Threshold (1/3)

- **Threshold value controls degree of grid refinement based on values of ω**
  - Decreased threshold yields increased grid density
  - Cases run at threshold values from 40 through 200 (12 jobs total)
  - Executed for 6,000 iterations – sufficient to understand grid resolution
  - Cartesian grid convergence observed after 5,000 iterations
- **Analysis performed at α = 2.75 deg. (plotted) and 4.25 deg.**

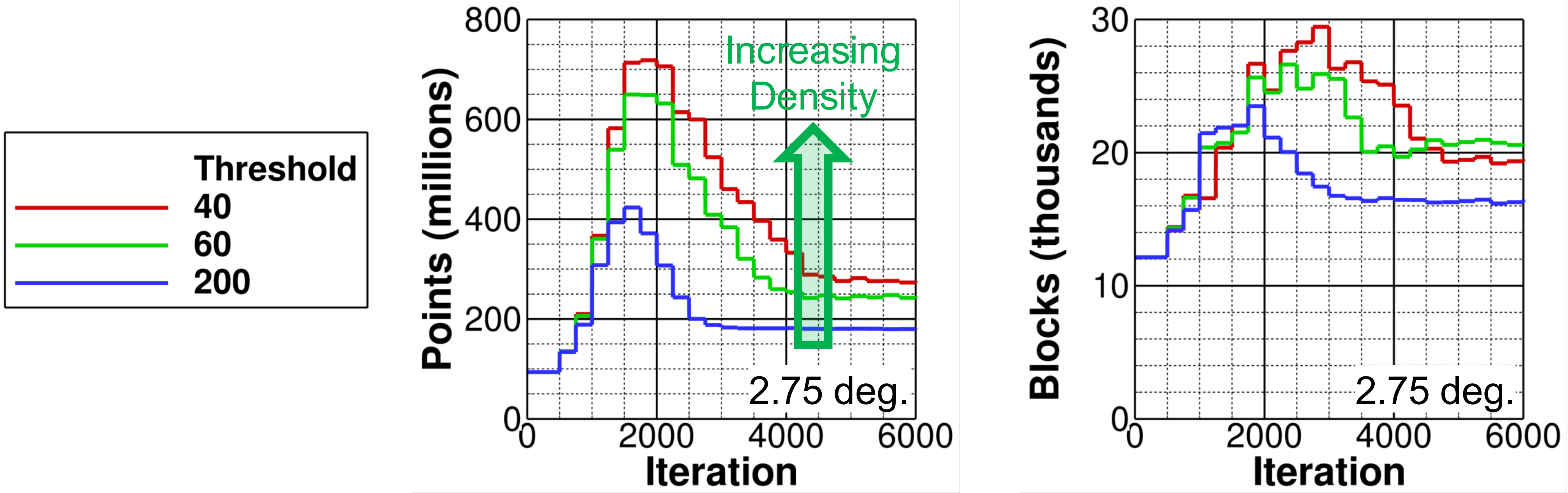

Case 4: Effect of Refinement Threshold (2/3)

- **Selection of threshold significantly affects wake refinement**
- **Chose threshold value of 60 with ~280 million cells in Cartesian region**
  - Minimal grid changes at α = 2.75 deg.
  - Adequately captures wing tip vortex, mid-span separation, and fuselage vortex

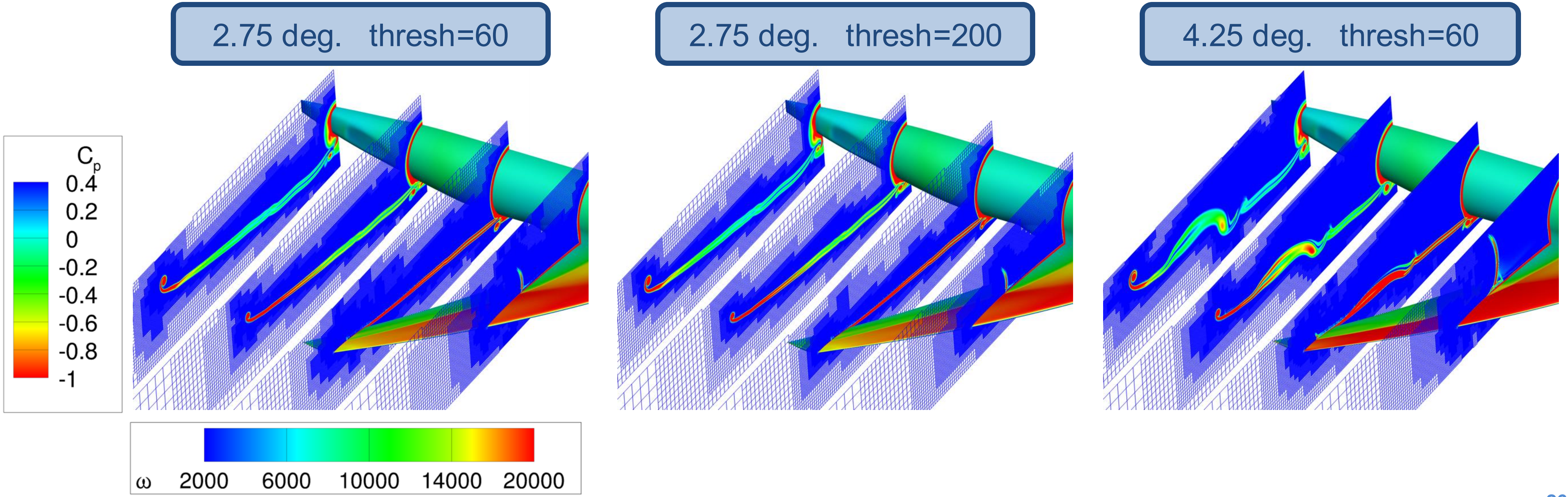

Case 4: Effect of Refinement Threshold (3/3)

- **Range of thresholds analyzed at C_L of 0.58**
- **Threshold value has minimal effect on F&M at this condition**
  - Consistent with expected results
  - Improved resolution of the wake and the shock
- **This observation does not mean that refinement has no effect on the global F&M (covered in next slides)**

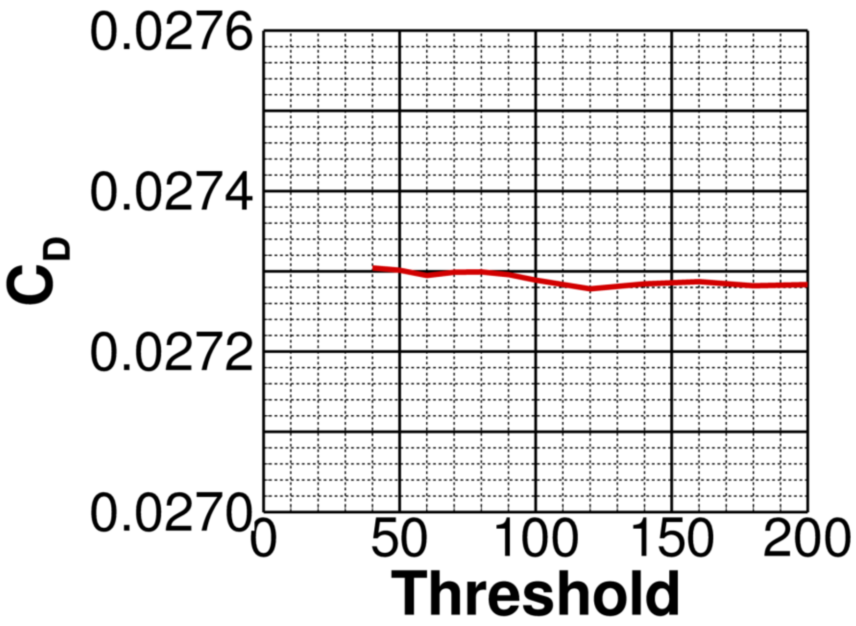

Case 4: Aerodynamic Performance

- **Adapted grid yields only a slight reduction in lift and moment magnitude**
- **Pitch-up break point extremely similar for both formulations**
- **Observations consistent with typical Kestrel behavior**

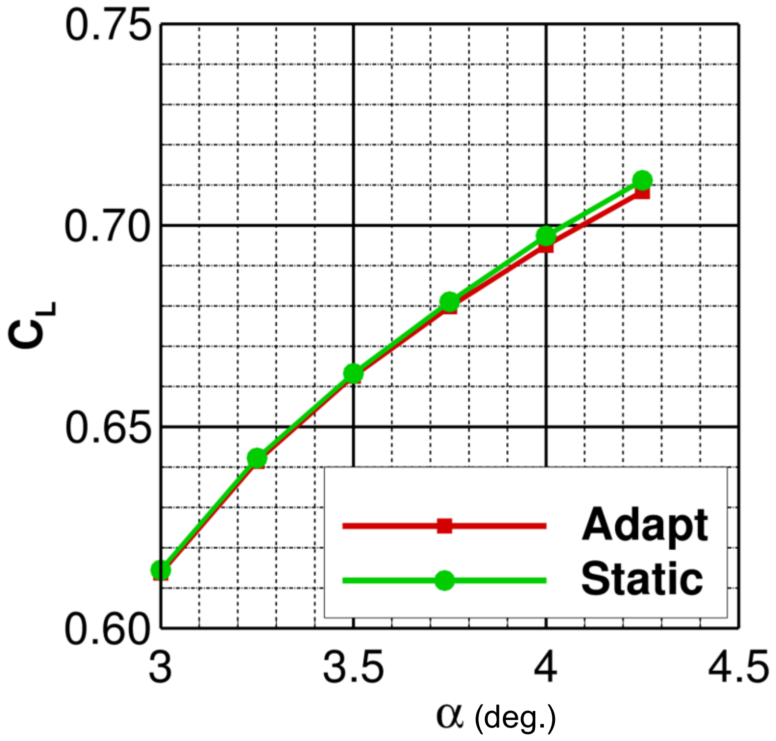

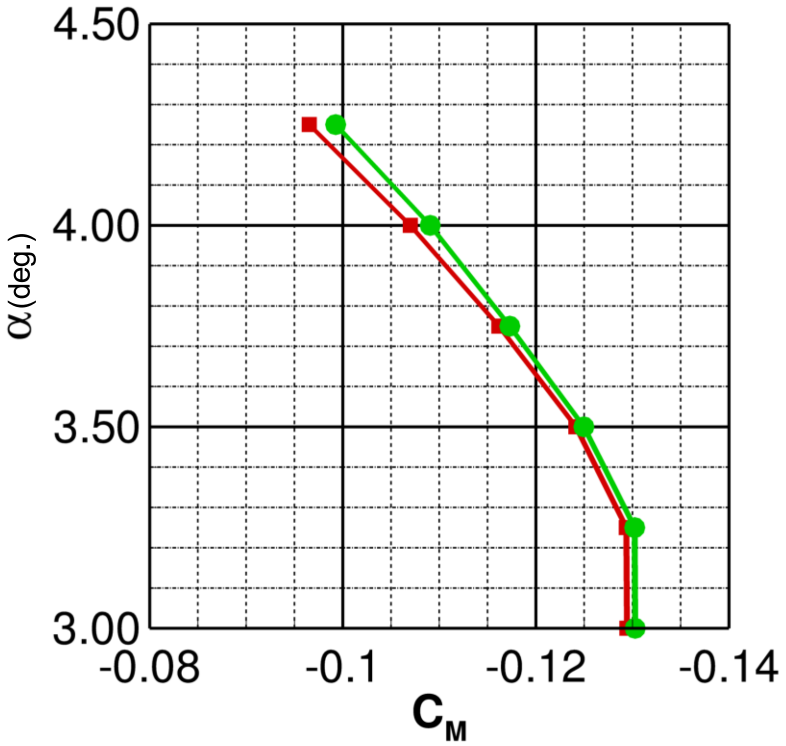

Case 4: Convergence History

- **Similar convergence history across full range**
- **Differences in averaged values**
  - Grid-adapted solutions yield decreased drag
  - C_L ~0.001
  - Maximum C_D delta ~3 counts

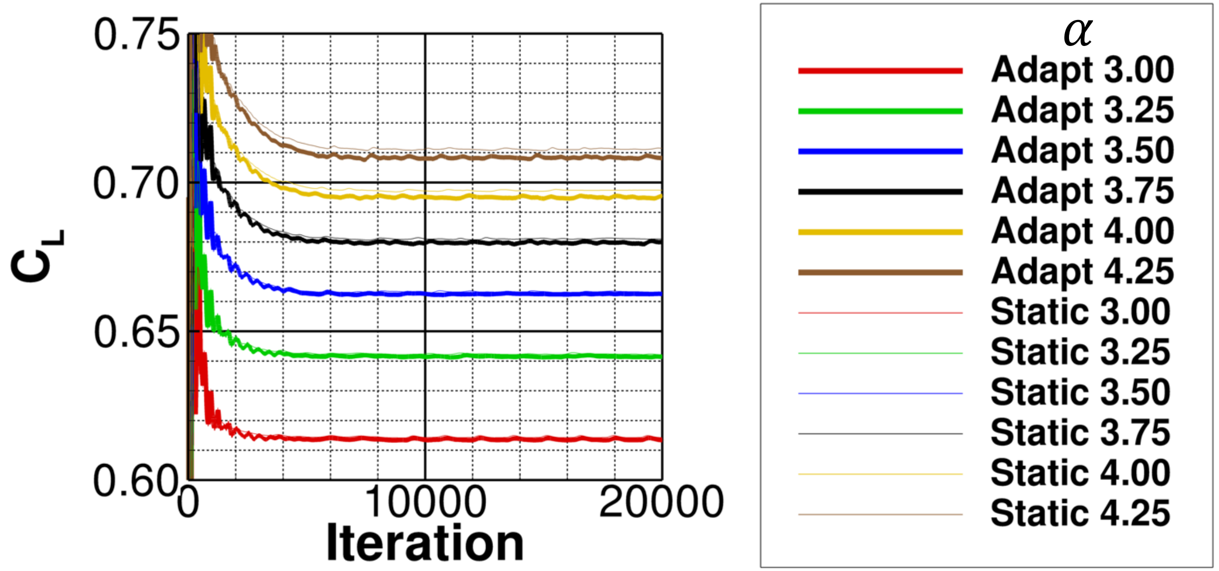

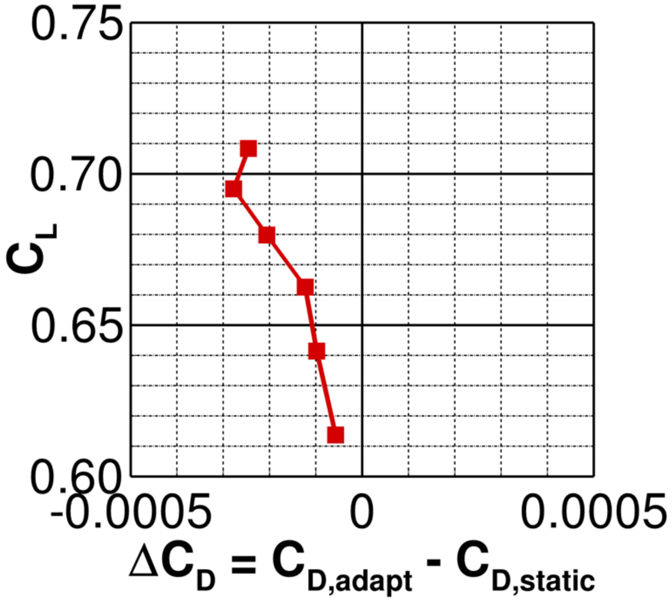

Case 4: Pressure Cuts (C_L 0.58)

- Overall, minimal changes observed in surface C_P data
- Slight forward movement of shock at outboard locations

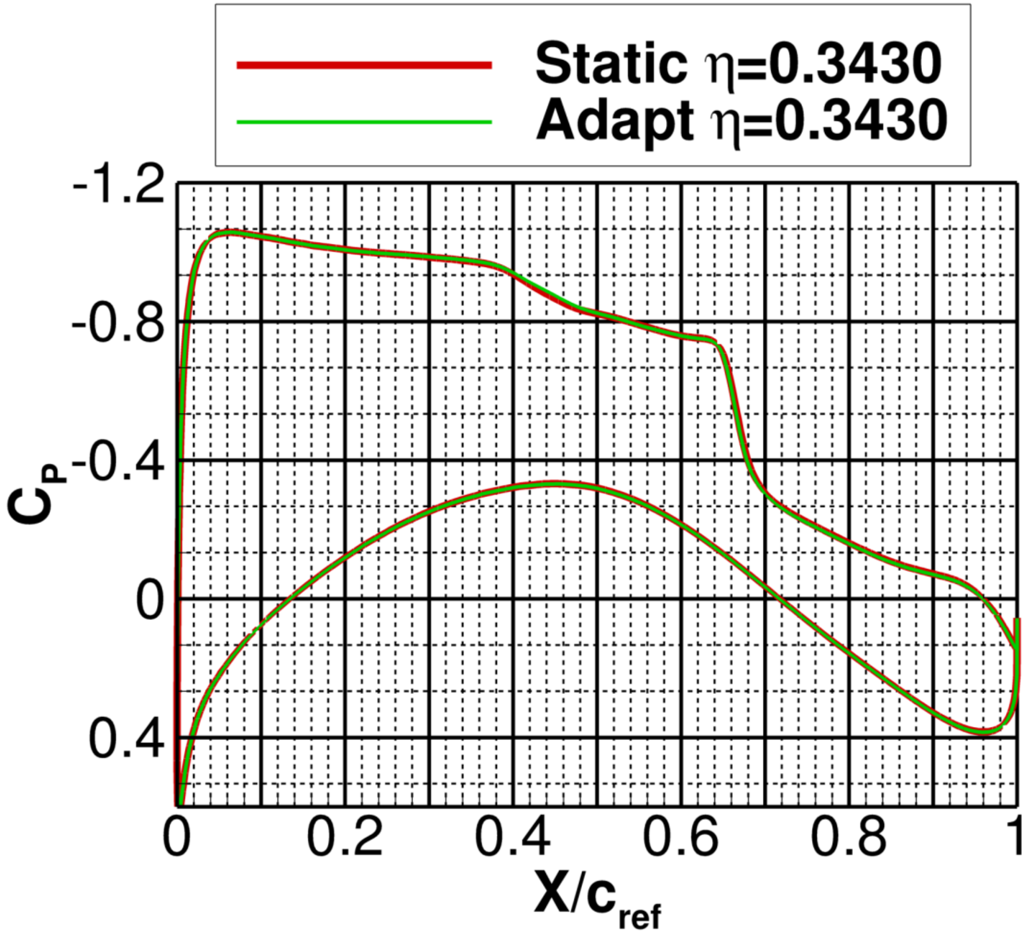

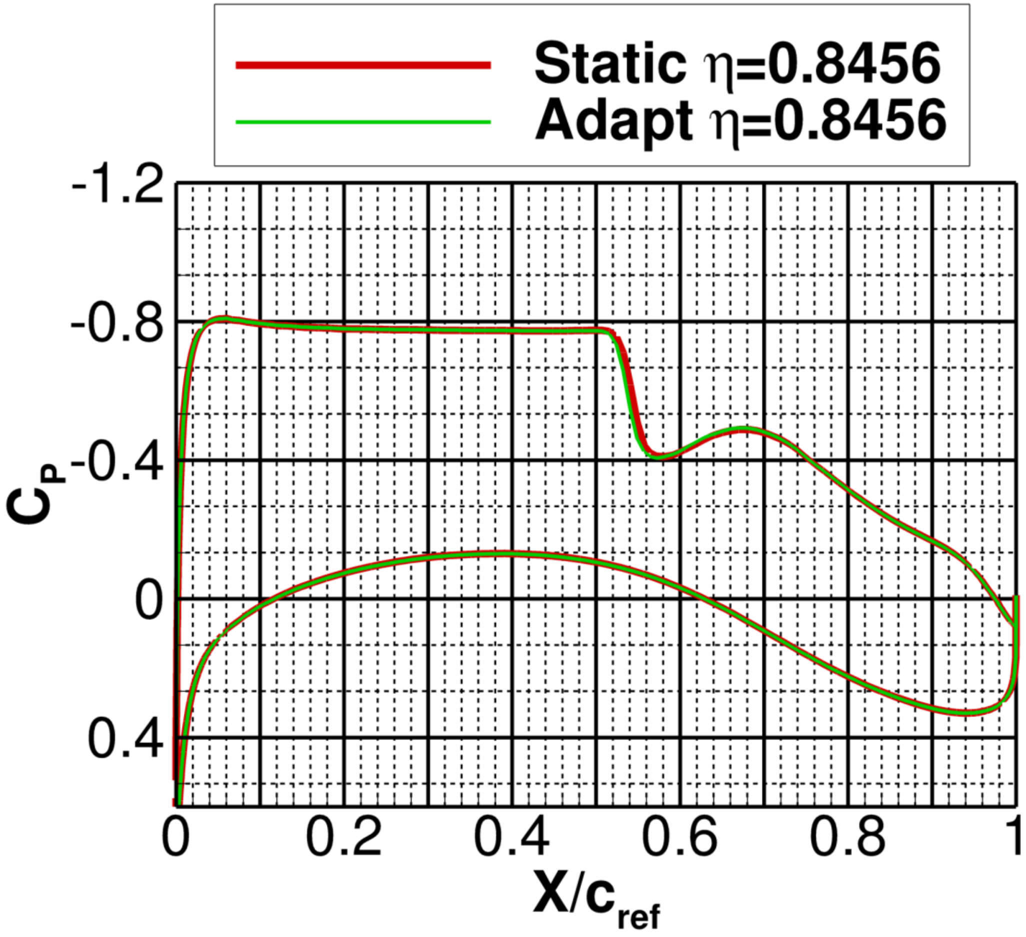

Case 5: Beyond RANS (DDES Adaptive Mesh)

- **Similar setup to RANS cases**
  - Same refinement region and settings
  - SARC-QCR turbulence model
- **Averaging window**
  - Simulation run for 26,000 iterations (not 20,000)
  - Began averaging at 20,000 iterations
  - Averaged for 6,000 iterations (not 2,000)
- **Nondimensional time step set to 0.010, dimensional time step falls out**

$$\frac{V_\infty \times dt}{c_{ref}} = dt^*$$

$$dt = \frac{dt^* \times c_{ref}}{V_\infty}$$

$$dt = \frac{0.010 \times 1.0}{7239.725}$$

$$dt = 0.000001381$$

Case 5: Beyond RANS (DDES Adaptive Mesh)

Case 5: Opportunities for Investigation

- **A more thorough investigation is warranted**
- **Grid considerations**
  - Appropriateness of current grids for DDES need to be investigated
  - Possibility of modeled stress depletion should be analyzed
- **Computational settings**
  - Temporal damping may need to be considered
  - Examine impact of RC and QCR
  - Smaller time steps might be significant

Summary

- Analysis performed on Cases 1a, 2a, 3, 4, and 5
- Excellent unstructured grid convergence achieved
- Pitch break observed C_L ~0.62
- Offbody adaptive mesh refinement improved wake prediction, but minimal effect on integrated F&M
- Unsteady DDES yielded earlier separation than RANS

Questions?